Vertical variability of near-surface salinity in the tropics: Consequences for L-band radiometer calibration and validation

Claire Hénocq, Jacqueline Boutin, François Petitcolin, Gilles Reverdin, Sabine Arnault, Philippe Lattes

Vertical Variability of Near-Surface Salinity in the Tropics: Consequences for L-Band Radiometer Calibration and Validation

CLAIRE HENOCQ,* JACQUELINE BOUTIN,+ FRANÇOIS PETITCOLIN,#,@ GILLES REVERDIN,+ SABINE ARNAULT,& AND PHILIPPE LATTES**

* *LOCEAN/IPSL, Paris, and ACRI-St, Sophia-Antipolis, France*
+ *LOCEAN/IPSL, and CNRS, Paris, France*
# *ACRI-St, Sophia-Antipolis, France*
& *LOCEAN/IPSL, and IRD, Paris, France*
** *LOCEAN/IPSL, Paris, France*

(Manuscript received 18 September 2008, in final form 26 June 2009)

ABSTRACT

Two satellite missions are planned to be launched in the next two years; the European Space Agency (ESA) Soil Moisture and Ocean Salinity (SMOS) and the National Aeronautics and Space Administration (NASA) Aquarius missions aim at detecting sea surface salinity (SSS) using L-band radiometry (1.4 GHz). At that frequency, the skin depth is on the order of 1 cm. However, the calibration and validation of L-band-retrieved SSS will be done with in situ measurements, mainly taken at 5-m depth. To anticipate and understand vertical salinity differences in the first 10 m of the ocean surface layer, in situ vertical profiles are analyzed. The influence of rain events is studied. Tropical Atmosphere Ocean (TAO) moorings, the most comprehensive dataset, provide measurements of salinity taken simultaneously at 1, 5, and 10 m and measurements of rain rate. Then, observations of vertical salinity differences, sorted according to their vertical levels, are expanded through the tropical band (30°S–30°N) using thermosalinographs (TSG), floats, expendable conductivity–temperature–depth (XCTD), and CTD data. Vertical salinity differences higher than 0.1 pss are observed in the Pacific, Atlantic, and Indian Oceans, mainly between 0° and 15°N, which coincides with the average position of the intertropical convergence zone (ITCZ). Some differences exceed 0.5 pss locally and persist for more than 10 days. A statistical approach is developed for the detection of large vertical salinity differences, knowing the history of rain events and the simultaneous wind intensity, as estimated from satellite measurements.

1. Introduction

Climate variability is closely linked to the global water cycle. Given the enormous volume of water contained in the ocean compared to the earth's other water reservoirs, the global water cycle is primarily driven by ocean–atmosphere exchanges (Schmitt 2008). Sea surface salinity (SSS) variations are strongly linked to precipitation over the ocean (representing nearly 379×10^3 km^3 yr^{-1} of freshwater) and evaporation (nearly 411×10^3 km^3 yr^{-1}). In that context, the introduction of salinity measurements in ocean circulation models is expected to provide a powerful method for estimating evaporation minus precipitation over the ocean (U.S. CLIVAR Office 2007). The measurements of SSS have also been shown to be valuable for describing, understanding, and improving the modeling of various oceanographic processes, as reviewed by Delcroix et al. (2005) and U.S. CLIVAR Office (2007). As a consequence, measuring SSS on a global scale is a major challenge for the oceanographic community.

Despite the increasing deployment of Argo floats and the increasing number of voluntary observing ships, the surface ocean coverage is uneven and limited (Bingham et al. 2002; Gould et al. 2004). Satellite measurements would provide synoptic and quasi-permanent surface ocean coverage; this is the main motivation to develop

@ Deceased.

Corresponding author address: Claire Henocq, Laboratoire d'Océanographie et du Climat par Expérimentation et Approches Numériques, Institut Pierre Simon Laplace, Unité mixte de Recherche CNRS/IRD/UPMC/MNHN, Université Pierre et Marie Curie, 4 place Jussieu, 75252 Paris CEDEX 05, France.
E-mail: claire.henocq@locean-ipsl.upmc.fr

DOI: 10.1175/2009JTECHO670.1

remote sensing of SSS (Lagerloef et al. 1995; Yueh et al. 2001). Two satellite missions, using L-band (1.4 GHz) radiometry for the detection of SSS, will be launched in the next two years. The European Space Agency (ESA) Soil Moisture and Ocean Salinity (SMOS) satellite mission will derive SSS on individual pixels with a spatial resolution at ground level of about 40 km and global surface ocean coverage of between 3 and 7 days (Barre et al. 2008). The accuracy expected on a single observation goes from 0.5 at the center of the swath to 1.7 practical salinity scale (pss) of 1978 at the edge on SSS, at 35 pss and 15°C (Zine et al. 2008). To reduce these uncertainties to a mean accuracy of 0.2 pss, SMOS SSS data will be averaged over 10 days and 200 km $\times$ 200 km (Boutin et al. 2004). The goal of the National Aeronautics and Space Administration (NASA) Aquarius mission is to retrieve SSS in the open ocean with a spatial resolution of about 150 km and an accuracy of 0.2 pss on a monthly basis (Le Vine et al. 2007).

Measuring salinity from space is very challenging because the sensitivity of brightness temperature (Tb) at L band to SSS is weak, on the order of 0.5 K pss^{-1}, and requires tightly controlled stability of the radiometer and accurate corrections for geophysical effects other than SSS. The calibration and validation of L-band radiometer measurements will therefore be a critical step. In particular, comparisons between in situ and retrieved SSS will be used to detect errors and biases in the retrieved SSS, linked to errors and biases in L-band radiometer Tb and/or in forward radiative transfer models. These data will be representative of the top 1 cm of the ocean surface, whereas Argo floats, the main source of in situ salinity data, do not measure salinity at a depth of less than 5 m (Riser et al. 2008). In most regions, salinity and temperature are homogeneous from the surface to several meters, but sometimes, especially during rain events, some vertical differences appear near the surface. In consequence, it is important to know and pay attention to the influence of rainfall on vertical salinity structure near the surface. It is interesting to underline that, from a radiometric point of view, salinity retrieval from L-band Tb should not be disturbed by rain rates lower than 10 mm h^{-1} (Peichl et al. 2005).

In the past, several local experiments have focused on observations of the effect of rain on SSS fluctuations, and several studies have tried to model this effect. Elliott (1974) attempted to evaluate the total precipitation from salinity changes, using data collected during the Barbados Oceanographic and Meteorological Experiment (BOMEX) in the summer of 1969. His results were inconclusive, because the local variability of salinity between 1 and 10 m, in the absence of rain events, is close to the salinity fluctuation caused by dilution resulting from rainfall (0.15 pss).

The depth and the vertical extent of salinity anomalies are very dependent on atmosphere–ocean interactions. The Tropical Ocean Global Atmosphere (TOGA) Coupled Ocean–Atmosphere Response Experiment (COARE) shows the diversity of salinity behavior according to the rain rate or wind speed. Soloviev and Lukas (1997) observed, in the center of equatorial Pacific Ocean during May 1994, a 0.5-pss freshening between the surface and 3 m (low wind speed and no estimation of the rain rate). By contrast, in the same region during December 1992, during a westerly wind burst, Wijesekera et al. (1999) demonstrated the presence of a freshening extending down from the surface to a depth of 40 m, with a horizontal variation at the surface of 0.12 pss in less than 20 km.

Models of the effect of rainfall on salinity have been developed and validated using in situ measurements. Miller (1976) developed a one-dimensional (1D) and time-dependent model based on conservation of heat and mechanical energy and on conservation of salt content. It determines the maximum depth of the freshening, its persistence, and the maximum temperature and salinity changes at the surface. This model, relevant in relation to the measurements made by Ostapoff et al. (1973), identifies the main characteristics of the effect of rainfall on salinity:

- Precipitation creates a new, shallower mixed layer, the so-called rain-formed mixed layer by Price (1979).
- Its depth increases with wind speed; for a given rate of precipitation, its depth increases with the duration of the rainfall.
- Changes in salinity and temperature cannot usually be detected under conditions of light precipitation and large surface wind speed. In contrast, in the equatorial Atlantic Ocean, heavy rainfall (more than 11 mm h^{-1}) with low wind speed (5 m s^{-1}) produces temperature and salinity decreases of 0.76°C and 2 pss, respectively, on a rain-formed mixed layer of 0.76 m (Miller 1976). In this case, the salinity ''jump'' at the bottom of the rain-formed mixed layer remains higher than 0.1 pss over 15 h.

More recently, Schlüssel et al. (1997) proposed to estimate the freshwater volume associated with rainfall that enters in the molecular sublayer of the ocean, taking into account the molecular diffusion and the behavior of raindrops according to their size (Hsiao et al. 1988). This model has been validated using TOGA COARE measurements showing about 3-pss anomalies in the first 2–3 cm associated with rain rate of about 10 mm h^{-1} and low wind speed.

The purpose of this paper is to investigate vertical salinity differences as recorded by widely available observations, to be used for satellite SSS calibration and validation, and to estimate the average biases expected from statistical comparisons between satellite SSS measurements in the top 1 cm and in situ measurements conventionally performed at 5–10-m depth. This paper focuses on the tropical region between 30°N and 30°S, because a preliminary work shows that absolute values of the vertical differences in salinity poleward of 30°N and 30°S are less than 0.1 pss. This result was also observed by Boutin and Martin (2006). The underlying objective is to propose new methods to optimize the calibration and validation of the L-band radiometer SSS measurements, such as, for instance, the determination of areas best suited for deploying a network of drifters measuring salinity in the first 10–50 cm below the surface (Reverdin et al. 2007) and to perform high-resolution vertical profiles with newly developed instruments, such as the Skin Depth Experimental Profiler [SkinDeEP; see Ward et al. (2004) for description and Ho et al. (2004) for results obtained in the Biosphere 2 ocean].

After a presentation of the measurements and the methods used, freshening resulting from rain events, their occurrence, and their persistence are described in the first part. Then, the response of the water column to a rain event through the tropical band is described and analyzed. The final part deals with a statistical description of widely spread observations relative to rain rate and surface wind speed and a discussion of its consequences for calibration and validation of the L-band radiometer SSS measurements.

2. Data and methods

a. Salinity measurements

In the following, the main characteristics of the datasets used are described. Thorough sortings and corrections are detailed in the appendix.

1) DESCRIPTION

The Tropical Atmosphere Ocean/Triangle Trans-Ocean Buoy Network (TAO/TRITON) project is an array of 70 moorings in the tropical Pacific Ocean [see full description online at http://www.pmel.noaa.gov/tao/; see also McPhaden (1995)]. This array was complemented in 1997 by several Pilot Research Moored Array in the Tropical Atlantic (PIRATA) moorings (Servain et al. 1998). Some of these moorings simultaneously provide vertical profiles of salinity and temperature, and precipitation and wind speed measurements. Hourly means of salinity measurements at 1, 5, and 10 m from TAO/PIRATA moorings are used between January 2000 and December 2006. The selection of valid data is made according to the validation flags provided on the Web site. In addition, a check on the consistency of vertical salinity profiles is performed (see the appendix). After this work, 13 sites are selected and analyzed (see positions and time periods on Table 1).

Temperature and salinity are measured by a thermosalinograph (TSG) on board the Research Vessel (R/V) *Polarstern* at 5-m and 11-m depth every 15 min. This ship crosses the Atlantic Ocean twice a year. The R/V *Polarstern* is not the only ship with TSG on board, but it is the only one that records two measurements at two different depths. The data used were collected from 1993 to 2005. As for the TAO/PIRATA measurements, a thorough work of data correction and sorting is necessary (see the appendix).

Argo measurements are downloaded from the Coriolis database [available online at http://www.coriolis.eu.org/cdc/argo.htm; see full description in Gould et al. (2004)]. Vertical profiles with at least two measurements of salinity between 1- and 11-m depths, from 1 January 2000 to 31 December 2006, are retained. The selection of Argo data is made depending on two criteria. First, a study about the method of sampling conductivity according to the type of floats leads us to consider only measurements from Autonomous Profiling Explorer (APEX) floats, which are the only ones that do not record a depth-integrated conductivity. Then, the selection is made in accordance with the Coriolis validation flags (Wong et al. 2008; see the appendix).

The World Ocean Database 2005 (WOD05; available online at http://www.nodc.noaa.gov/OC5/SELECT/dbsearch/dbsearch.html; see Boyer et al. 2006) contains quality-controlled conductivity–temperature–depth (CTD) and expendable CTD (XCTD) ocean profiles collected since 1961. To be consistent with the temporal distribution of Argo floats, only salinity measurements made after 1 January 2000 between 4 and 11 m and higher than 20 pss are retained.

The Système d'Information Scientifique pour la Mer (SISMER) database provides also CTD measurements mainly conducted in the Gulf of Guinea and to the east of Indonesia (data available online at http://www.ifremer.fr/sismer/FR/donnees_FR.htm). The Altimétrie sur un Rail Atlantique et Mesures In Situ (ARAMIS) project (Arnault et al. 2004) uses a merchant ship along the AX11 route (35°N, 20°W to 20°S, 40°W). Twice a year, from 2002 to 2006, salinity and temperature are measured with a spatial resolution of 1° latitude by XCTD with a vertical resolution of 1 m. Data are processed by the ARAMIS team and only measurements below 4-m depth are considered.

TABLE 1. Location and time distribution of selected TAO moorings.

	Lat	Lon	Time availability	Depth taken into account
TAO moorings	0°	140°W	May–November 2004	1, 5, and 10 m
			November 2004–February 2005	5 and 10 m
			February–May 2005	1, 5, and 10 m
	0°	110°W	April–August 2005	5 and 10 m
			November 2005–April 2006	1, 5, and 10 m
	12°N	95°W	April 2000–July 2001	1, 5, and 10 m
	10°N	95°W	November 2000–December 2001	1, 5, and 10 m
			December 2002–November 2003	1 and 5 m
	8°N	95°W	April 2000–March 2001	1, 5, and 10 m
			November 2001–February 2002	1, 5, and 10 m
			October 2002–May 2003	1, 5, and 10 m
	5°N	95°W	November 2000–May 2003	1, 5, and 10 m
	3.5°N	95°W	April–July 2000	5 and 10 m
			May–August 2001	1, 5, and 10 m
			October 2002–November 2003	1, 5, and 10 m
	2°N	95°W	April 2000–June 2001	1, 5, and 10 m
	0°	95°W	April 2000–January 2001	1, 5, and 10 m
			October 2001–February 2003	1, 5, and 10 m
	2°S	95°W	April–November 2000	1, 5, and 10 m
			November 2001–March 2002	1 and 5 m
			October 2002–April 2003	1, 5, and 10 m
	5°S	95°W	November 2001–July 2002	1, 5, and 10 m
	8°S	95°W	October 2001–March 2002	1, 5, and 10 m
			October 2002–January 2003	5 and 10 m
PIRATA mooring	12°N	23°W	June–October 2006	1 and 10 m

2) THE ENSEMBLE DATASET

For each vertical profile, the vertical salinity difference is computed between two levels as deepest minus shallowest salinity measurement. The vertical sampling of salinity measurements is different, depending on the various types of platforms. To organize the analysis, the vertical differences are ranked in three groups (referred to in what follows as vertical levels):

$$\Delta S_{10-5} = S[8;\ 11]\,\mathrm{m} - S[4;\ 6]\,\mathrm{m},$$

meaning that the difference between salinity measured between 8 and 11 m and salinity measured between 4- and 6-m depth is computed;

$$\Delta S_{5-1} = S[4;\ 6]\,\mathrm{m} - S[0;\ 2]\,\mathrm{m}; \quad \text{and}$$
$$\Delta S_{10-1} = S[8;\ 11]\,\mathrm{m} - S[0;\ 2]\,\mathrm{m}.$$

Nearly 280 000 vertical salinity differences are obtained over the entire tropical region (30°N–30°S). Note that 48% of vertical salinity differences included in ΔS_{10-5} come from TAO/PIRATA measurements, whereas ΔS_{5-1} and ΔS_{10-1} groups are based only on TAO/PIRATA measurements and more than 93% (82%) of the ΔS_{5-1} (ΔS_{10-1}) groups are located at 95°W. The different regions sampled by the various types of data are indicated in the appendix, as well as the distributions according to the data type, the vertical level, and the geographical location.

b. Collocated rain and surface wind speed measurements and salinity dataset

The influence of rainfall on vertical salinity differences is analyzed by using rain rates retrieved from satellite microwave radiometers: the Special Sensor Microwave Imager (SSM/I), the Tropical Rainfall Measuring Mission (TRMM) Microwave Imager (TMI), and the Advanced Microwave Scanning Radiometer (AMSR), delivered by Remote Sensing Systems [RemSS; available online at http://www.ssmi.com/; see description of the algorithm in Wentz and Spencer (1998) and description of the data in the appendix]. We also used wind speed retrieved from the same satellites measurements and Quick Scatterometer (QuikSCAT) measurements.

Satellite instruments provide two instantaneous ''snapshots'' each day with no indication of the start time of the rain event, its duration, and its overall intensity; however, the key information for predicting sea surface freshening is the rain history. Hence, we derive a rain parameter called the 3-day maximum accumulation rain rate (3d max rain rate) as the sum of the daily maximum rain rate measured by satellite over 3 days at each geographic location. The choice of 3 days was made because it ensures a quasi-global coverage of the satellite; using

2 days reduced the number of collocations by 10%, whereas the observed tendencies were very similar. Salinity vertical differences are collocated with the 3d max rain rate computed over the previous 72 h in 25-km radii. Salinity vertical differences have also been collocated with the maximum surface wind speed computed over the previous hour in 25-km radii (referred to here as 1hr_WS).

To remove anomalous vertical salinity differences related either to inaccurate measurements or coastal river discharge, a final selection based on a ''5 standard deviation'' criterion is applied (see the appendix).

c. *Statistical analysis*

To draw a statistical relation between vertical salinity differences and rainfall, a least squares regression line is computed for the whole dataset and for each vertical level. The resulting linear trends, vertical salinity differences in function of the 3d max rain rates, are superimposed on the mean and the standard deviation computed for each 2 mm h^{-1} group of 3d max rain rate.

To estimate the consistency of the statistical results obtained from various vertical levels, the sum of the linear trends of ΔS_{10-5} and ΔS_{5-1} is compared to the ΔS_{10-1} linear trend. More than 60% of vertical salinity differences included in ΔS_{10-5} does not come from the same profiles as the differences included in ΔS_{10-1} and ΔS_{5-1}.

To improve these statistical results, dependency on 1hr_WS is taken into account. The average on the whole associated 1hr_WS equals 6.1 m s^{-1}; the distinction of high and low 1hr_WS is made in accordance with this average. Then, the least squares regression lines are computed, distinguishing the intensity of 1hr_WS.

3. The SSS vertical differences as observed on TAO moorings

The temporal evolution of salinity during a rain event can be observed using measurements from the TAO project. On some moorings, measurements of temperature and salinity are performed every hour in the upper ocean at 1-, 5-, and 10-m depths. Measurements of precipitation are also performed every 10 min. In the following, the influence of rain events on salinity in the upper 10 m is illustrated on two distinct TAO moorings. These are located at 5°S, 95°W and at 10°N, 95°W and are referred to here as the 5S-95W and the 10N-95W TAO moorings, respectively. The analyzed time series of the 5S-95W TAO mooring extends from 16 to 20 February 2002. For the 10N-95W TAO mooring, the time series extends from 18 to 23 September 2001 (see Fig. 1).

During these periods, several rain events were followed by a decrease of salinity at 1 m. On 17 February 2002, the 5S-95W TAO mooring has registered several rain events with precipitation rates from 2.3 to 7.6 mm h^{-1} (durations of rain events go from 30 to 100 min). These events have no impact on salinity at 5 and 10 m and create only a freshening of less than 0.1 pss at 1 m. Conversely, on 18 February 2002, between 0950 and 1610 UTC, a rain event of 390 min with a mean precipitation rate of 7.8 mm h^{-1} is recorded, and it is followed by a maximum freshening of 0.93 pss at 1 m (reached at the end of the rain event) and a freshening of 0.35 pss at 5 m. Then, salinity at 1 and 5 m slowly recovers until the beginning of a new small rain event (mean precipitation rate equals 2.4 mm h^{-1} for a duration of 30 min). At that time, only salinity at 1 m registers another decrease of 0.14 pss. During this whole period, salinity at 10 m does not record any variation and remains between 34.71 and 34.73 pss.

Observations on the 10N-95W TAO mooring are similar. Three freshenings higher than 0.1 pss at 1 m are recorded: one decrease of salinity at 1 m of 0.18 pss, associated with a 190-min rain event and a mean precipitation rate of 6.4 mm h^{-1}; then, one of 1.67 pss (mean precipitation rate of 13.3 mm h^{-1} during 170 min); and one of 0.59 pss on the evening of 21 September (mean precipitation rate of 25.4 mm h^{-1} during 110 min). The salinity at 5 and 10 m is not influenced. During these freshening events, wind speed stays close to 4 m s^{-1}.

Vertical salinity differences observed on TAO moorings begin in late afternoon and end in early morning, which is consistent with the diurnal salinity cycle studied by Cronin and McPhaden (1999). These periods are within the time passage of SMOS and Aquarius (at 0600 and 1800 LT each day). The variety of the observed salinity fluctuations at 1 m, associated with a given rain rate, shows the difficulty of obtaining precise prediction on vertical salinity differences, taking into account only information on precipitation. Assuming an isohaline mixed layer and neglecting advection, the analysis indicates that salinity fluctuations cannot be solely explained by dilution processes. Between 0950 and 1610 UTC 18 February 2002, the total accumulated rain equals 50.6 mm. Given the background salinity of 34.68 pss and the observed freshening of 0.93 pss at 1 m, we estimate a rain-formed mixed layer of 1.85-m depth. This is consistent with freshening observed at 1-m depth, but not with the one occurring at 5-m depth. On 18 September 2001, the total rain amount of 37.8 mm, given a background salinity of 33.75 pss and a freshening of 1.64 pss, would correspond to a rain-formed mixed layer of 0.74-m depth, which is inconsistent with freshening observed at 1 m. A simple 1D homogeneous rain-formed mixed layer is not consistent with the observations; other processes,

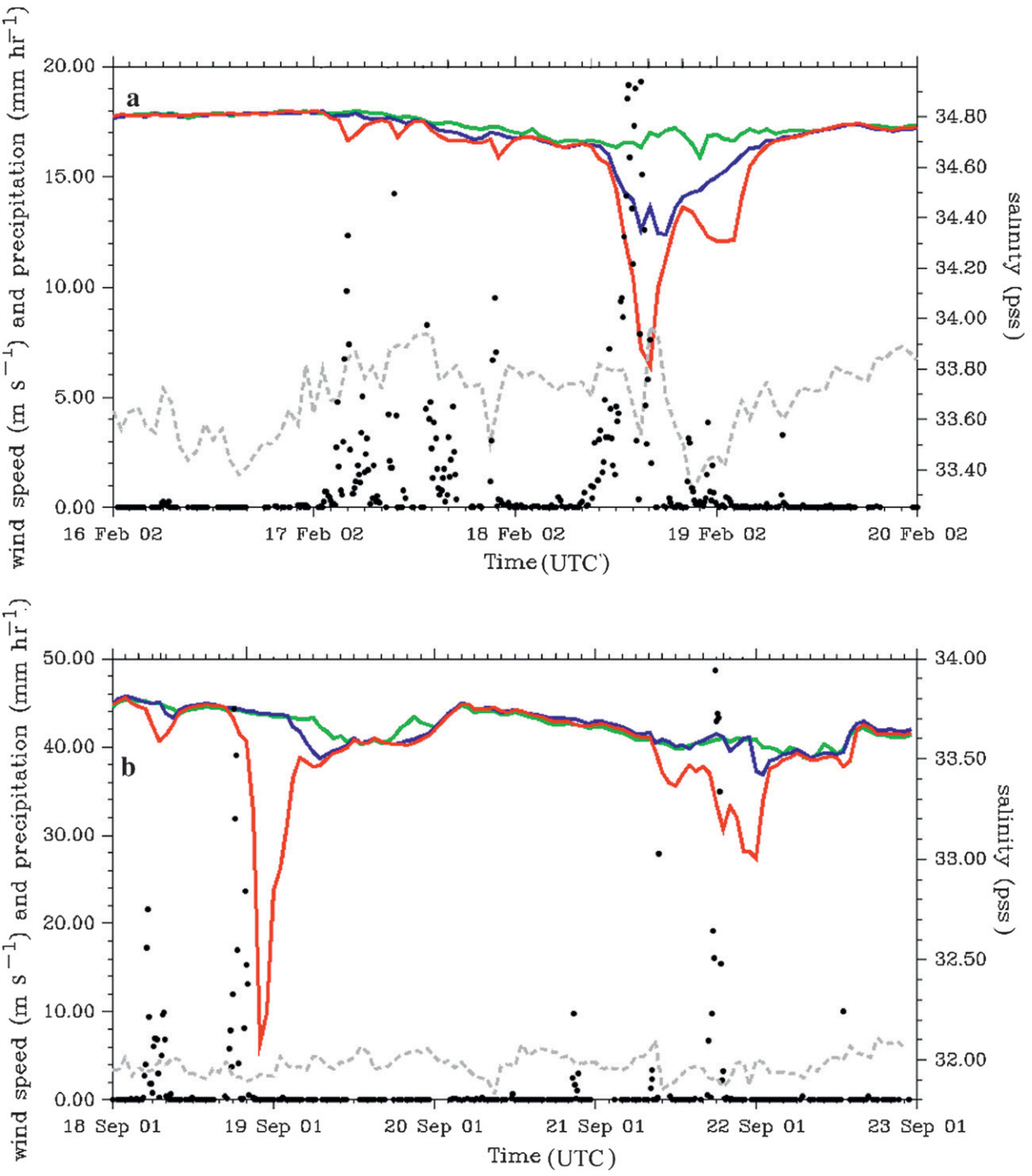

FIG. 1. The influence of rainfall and wind speed on salinity at 1 m measured by (a) 5S-95W and (b) 10N-95W TAO moorings. Salinity measurements taken at 1-m depth are represented by the red curve, salinity measurements at 5-m depth are represented by the blue curve, and salinity measurements at 10-m depths are represented by the green curve. The black dots represent the rain rate measured every 10 min and the gray dotted line represents the hourly mean wind speed.

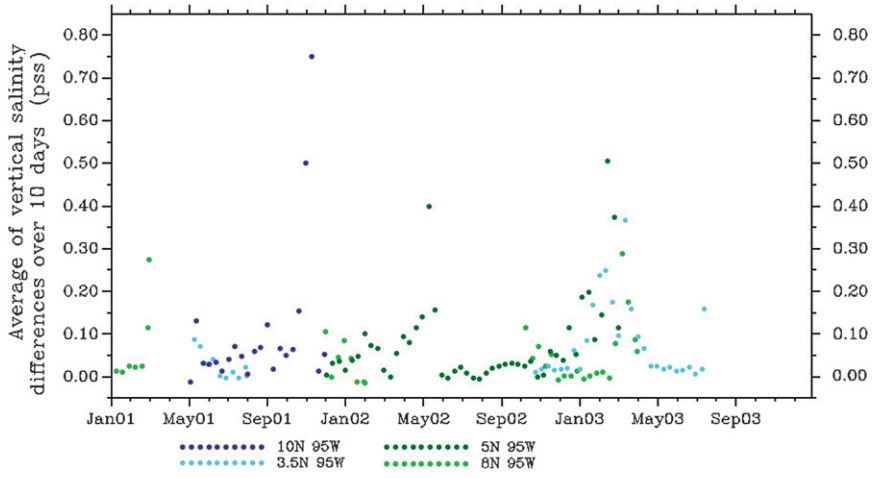

FIG. 2. The average of vertical salinity differences between 10- and 1-m depths over 10 days for four TAO moorings. Each color represents a different mooring.

such as horizontal advection of low salinity patches, are clearly important.

These freshening events (i.e., the salinity difference between 10 and 1 m remaining higher than 0.1 pss during more than 1 h) are not rare. On the 5S-95W mooring, 22 freshening events are observed, with half of them for less than 10 h. Altogether, freshening events appear during 329 h on a total of 5058 h of data (nearly 6.50% of temporal distribution). This result is very dependent on the geographical location of TAO moorings and goes from 0% (at 0°N, 140°W) to nearly 22% (at 10°N, 95°W) of temporal distribution. The same event can persist during several days. The maximum persistence time observed on TAO moorings equals 144 h for a mean vertical salinity difference between 10 and 1 m of 0.85 pss. On average over 10 days, these vertical salinity differences can reach 0.5 pss (see Fig. 2). Even if the geographical extent of a rain event rarely equals 200 km × 200 km, mixing and ocean surface currents can spread freshwater, stretch, and create artificial biases between L-band radiometer and in situ salinity measurements.

4. Vertical salinity differences through the tropical band

Vertical salinity differences greater than 0.1 pss are observed in each ocean, mainly between 0° and 15°N for the Atlantic and Pacific Oceans, throughout the Gulf of Bengal, and around the Indian coast (see Fig. 3a). These zones of high differences coincide with the average position of the intertropical convergence zone (ITCZ) and of the northern Indian Ocean monsoon, so they are likely related to precipitation. Isolated large differences near coastlines and river mouths (e.g., the Amazon River along the Brazilian coast, the Congo and Niger along the African coast, and the Gulf of Mexico) are observed.

However, salinity differences averaged either for each ocean or for each vertical level remain less than 0.05 pss (see Table 2). The percentage of salinity differences higher than 0.1 pss is small: over the whole database, 97.1% of salinity differences fall between −0.1 and 0.1 pss. Only 0.2% is below −0.1 pss, and 2.7% is higher than 0.1 pss. However, the percentage of high salinity differences increases when the shallowest measurement is taken at 1-m depth: salinity differences higher than 0.1 pss represent 7.13% for ΔS_{5-1} and 10.27% for ΔS_{10-1}, whereas they represent only 4.24% for ΔS_{10-5} (see Fig. 4a).

The positions of high 3d max rain rates coincide with positions of high salinity differences, especially in the Atlantic Ocean (see Fig. 3b). The comparison of mean, standard deviation, and distribution of high salinity differences between low 3d max rain rate (below 10 mm h^{-1}) and high 3d max rain rate (above 10 mm h^{-1}) shows clearly the link between precipitation and vertical salinity differences (see Table 2 and Fig. 4b).

This link is even clearer if average salinity differences are computed in 2 mm h^{-1} classes of 3d max rain rate (see Fig. 5): the larger the rain rate, the greater the vertical salinity differences. This appears both on average computed by 3d max rain rate classes and on regression lines computed from nonaveraged collocated data. Looking only at the vertical level, ΔS_{10-1} is always higher on average than ΔS_{5-1} and ΔS_{10-5}. The value of ΔS_{10-1} exceeds 0.1 pss on average for a rain rate higher than 5 mm h^{-1}.

The comparison between the different slopes of the linear trends for the three vertical levels shows the validity

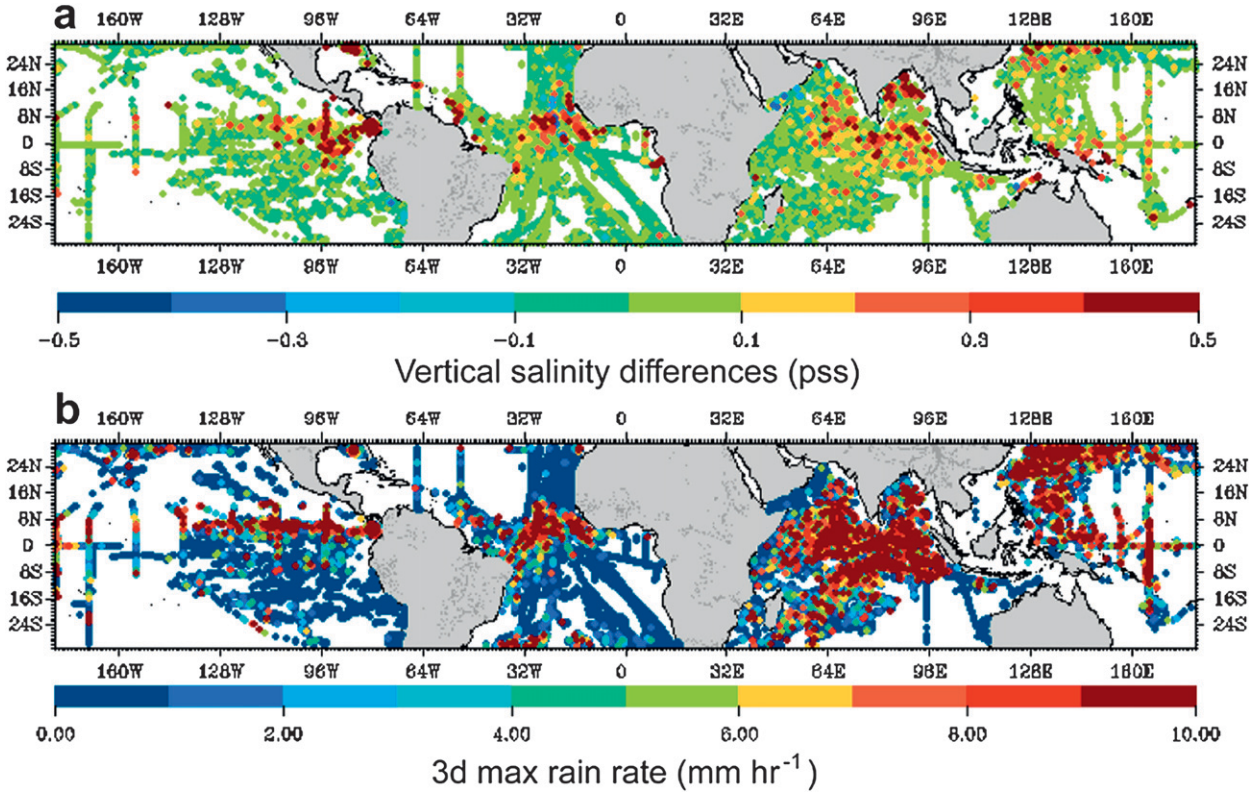

FIG. 3. The spatial distribution of (a) vertical salinity differences, all vertical levels confounded, and (b) 3d max rain rate associated with each salinity difference. The color bar in (a) indicates the value of vertical salinity differences (pss), and the color bar in (b) indicates the 3d max rain rate (mm h^{-1}). To draw attention to the extremes, when several values of vertical salinity differences (and, as a consequence, several values of 3d max rain rate as well) occur at the same point, only the highest absolute values are displayed.

of this statistical approach. Although more than 60% of vertical salinity differences included in ΔS_{10-5} does not come from the same profiles as the salinity differences included in ΔS_{10-1} and ΔS_{5-1}, the sum of the linear trends of ΔS_{10-5} and ΔS_{5-1} is very close to the ΔS_{10-1} linear trend (see Fig. 5).

The influence of wind speed is also considered; 37% of the dataset has been collocated with 1hr_WS. The linear

TABLE 2. Mean and standard deviation of vertical salinity differences according to their vertical levels, their geographical locations, and the intensity of 3d max rain rates.

	Mean of vertical salinity differences (pss)	Std dev of vertical salinity differences (pss)	No. of measurements
Over the whole dataset	0.027	0.109	277 907
Vertical level:			
ΔS_{10-5}	0.016	0.096	129 176
ΔS_{5-1}	0.029	0.098	85 737
ΔS_{10-1}	0.046	0.142	62 994
Geographical location:			
Atlantic Ocean	0.007	0.111	40 147
Pacific Ocean	0.031	0.111	22 438
Indian Ocean	0.010	0.064	13 402
Intensity of rain:			
3d max rain rate not computed*			2611
3d max rain rate < 10 mm h^{-1}	0.019	0.068	269 703
3d max rain rate ≥ 10 mm h^{-1}	0.085	0.168	5593

* 3d max rain rate is not computed when vertical salinity differences could not be collocated with any satellites measurements over the previous 72 h.

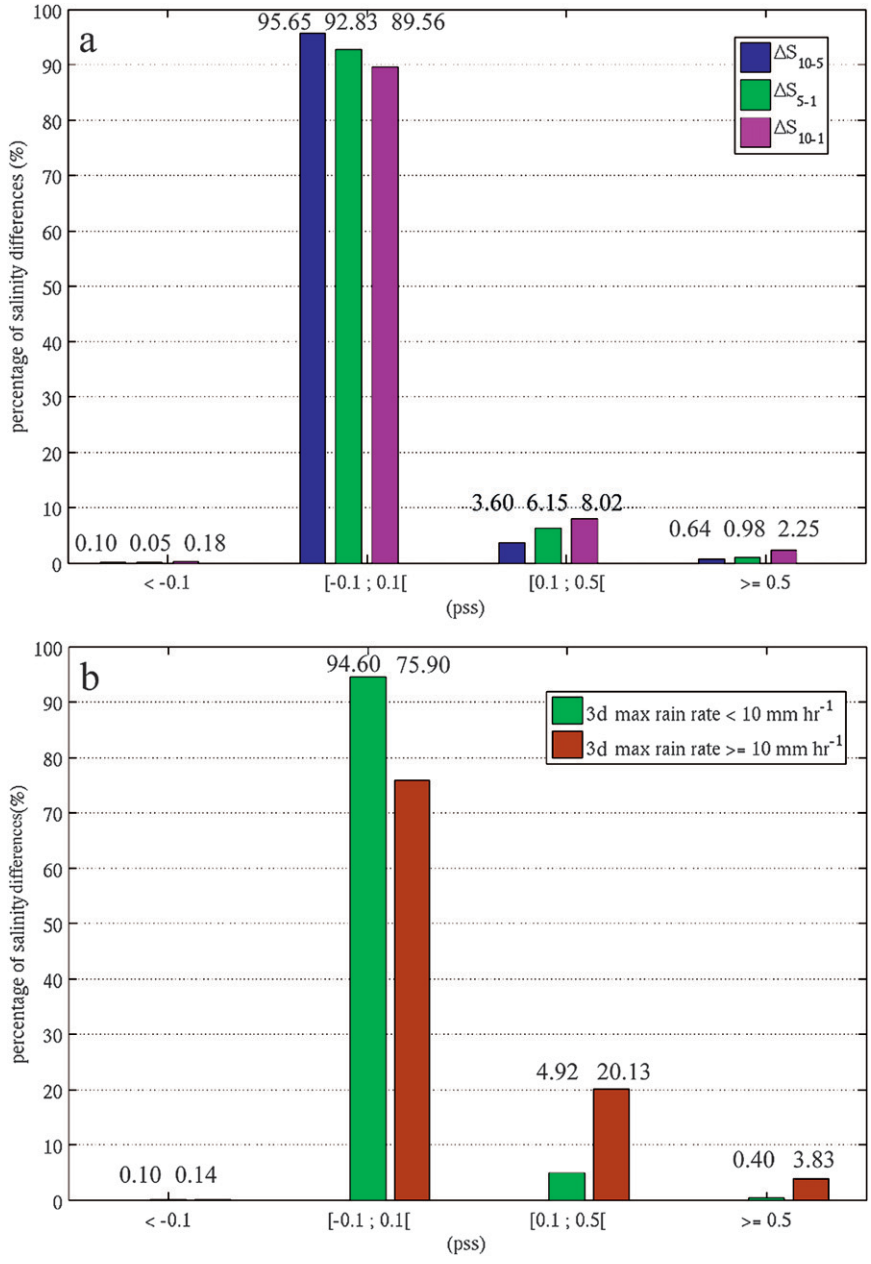

FIG. 4. The distribution of low, near-zero, and high vertical salinity differences according (a) to their vertical levels and (b) to the intensity of the 3d max rain rate.

trends displayed in Fig. 5 can be revisited by adding information on the intensity of 1hr_WS. For a given 3d max rain rate, the difference between vertical salinity gradients associated with low 1hr_WS and high 1hr_WS can reach 0.05 pss (see Fig. 6) and vertical salinity differences increase conversely with wind speed.

Our statistical approach, which is based on salinity collocated with satellite rain rate at 25-km resolution, provides a mean to empirically compute the salinity integrated over 25 km × 25 km at a shallower depth, knowing salinity at one depth. SMOS resolution will be slightly larger (on the order of 30 km × 30 km to 50 km × 50 km; Font et al. 2004); however, given that this statistical analysis does not take into account possible vertical differences between 1 cm and 1 m, this computation gives an order of magnitude of the expected difference between SMOS salinities and deeper measurements. From the equations of linear trends, if SX_m represents the salinity at X m and 3d_MRR (mm h^{-1}) represents the 3d max rain rate, an estimate of the salinity profile can be computed by

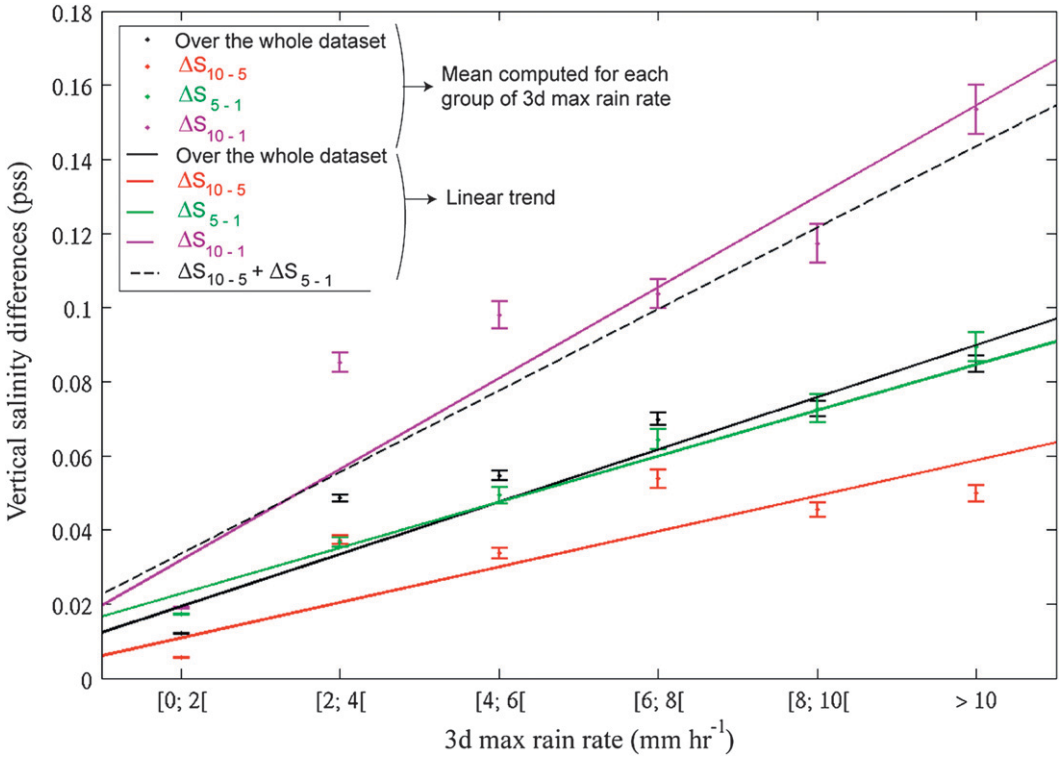

FIG. 5. The mean and standard deviation of salinity differences computed in 2 mm h^{-1} 3d max rain rate classes and the linear trends of vertical salinity differences vs 3d max rain rate computed from non-averaged data (black dots and curve). The same parameters are displayed for the different vertical levels (red for ΔS_{10-5}, green for ΔS_{5-1}, and purple for ΔS_{10-1}). Error bars represent the mean ± one standard deviation of vertical salinity gradients for each class of 3d max rain rate. The black dotted curve represents the comparison between the linear trend associated with ΔS_{10-1} (purple curve) and the linear trend associated with $\Delta S_{10-5} + \Delta S_{5-1}$.

$$\text{S10\_m} - \text{S5\_m} = (0.005 \pm 0.10\,10^{-3}) \times \text{3d\_MRR} + (0.006 \pm 0.35\,10^{-3}), \quad (1)$$

$$\text{S5\_m} - \text{S1\_m} = (0.006 \pm 0.20\,10^{-3}) \times \text{3d\_MRR} + (0.017 \pm 0.50\,10^{-3}), \quad \text{and} \quad (2)$$

$$\text{S10\_m} - \text{S1\_m} = (0.012 \pm 0.25\,10^{-3}) \times \text{3d\_MRR} + (0.020 \pm 0.75\,10^{-3}). \quad (3)$$

Each associated 95% confidence interval, calculated using a standard t test, is indicated in parentheses. In the case that 1hr_WS (m s^{-1}) is known, a multiplying coefficient is computed to model the influence of wind speed. The linear least squares regressions turn into

$$\text{S10\_m} - \text{S5\_m} = \frac{(0.005 \pm 0.20\,10^{-3}) \times \text{3d\_MRR}}{1 + (-0.188 \pm 6.50\,10^{-3}) \times \text{1hr\_WS}} + (0.005 \pm 0.47\,10^{-3}), \quad (4)$$

$$\text{S5\_m} - \text{S1\_m} = \frac{(0.005 \pm 0.29\,10^{-3}) \times \text{3d\_MRR}}{1 + (-0.250 \pm 0.02) \times \text{1hr\_WS}} + (0.016 \pm 0.75\,10^{-3}), \quad \text{and} \quad (5)$$

$$\text{S10\_m} - \text{S1\_m} = \frac{(0.012 \pm 0.46\,10^{-3}) \times \text{3d\_MRR}}{1 + (-0.243 \pm 0.03) \times \text{1hr\_WS}} + (0.017 \pm 1.10\,10^{-3}). \quad (6)$$

5. Discussion

The comparison between the different vertical levels indicates the necessity of taking into account the depth in situ data for the calibration and validation of satellite measurements in rainy regions; the highest salinity differences occur when the shallowest measurement is taken at 1 m. At local scale, ΔS_{5-1} can reach 1 pss. The 3d max rain rate appears to be a reliable parameter for the detection via statistical methods of the salinity differences between surface L-band radiometer measurements and in situ measurements resulting from rainfall.

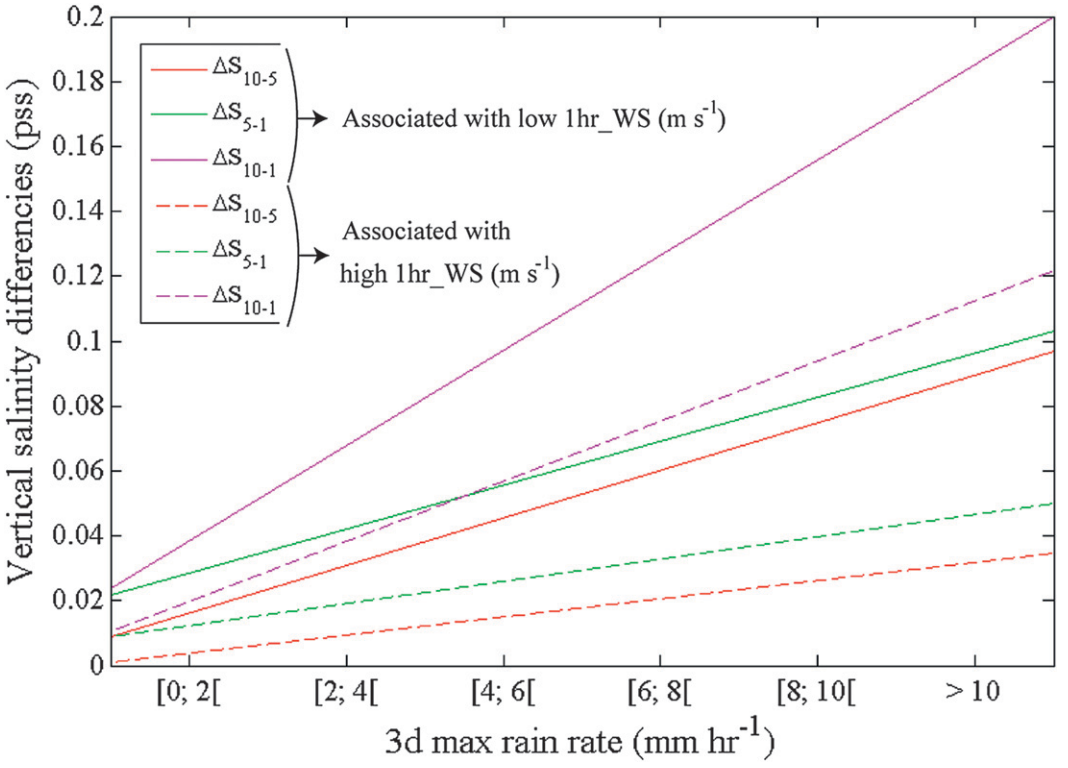

FIG. 6. Linear trends of vertical salinity differences vs 3d max rain rate computed from non-averaged data according to their different vertical levels (red for ΔS_{10-5}, green for ΔS_{5-1}, and purple for ΔS_{10-1}) and according to the intensity of 1hr_WS. The dotted lines represent vertical salinity differences associated with high 1hr_WS (higher than 6.1 m s^{-1}) and the continuous lines represent vertical salinity differences associated with low 1hr_WS.

However, more than 75% of vertical salinity differences comes from 13 fixed positions in the tropics (TAO/TRITON and PIRATA moorings), mainly located at 95°W. More measurements above 5 m are urgently needed to extend and improve this work.

This paper focuses on vertical salinity differences between 1 and 10 m. In the case of a rain-formed mixed layer deeper than 1 m, the least square relations found can be used in comparison between L-band-retrieved salinity and in situ salinity. Otherwise, the largest differences are expected to occur between 1 cm and 1 m but are difficult to estimate, because measurements are rare in the uppermost meter. Some surface floats have recently been deployed to measure temperature and salinity near the surface. For instance, Metocean drifters provide series of conductivity and temperature measurements at hourly intervals at 50-cm depth (see description in Reverdin et al. 2007). One Metocean buoy, deployed near the Amazon estuary in October 2007, recorded a significant decrease in salinity during the night from 29 to 30 December 2007, from 35.76 to 35.06 pss (see Fig. 7). The salinity recovers its initial value 14 h later. The *F14* and *F13* SSM/I satellite sampled the same area as the MetOcean drifter on 29 December 2007, at the beginning of the SSS decrease event, at 2036 and 2111 LT, respectively. They show the occurrence and the persistence of a rain event for more than 40 min (see Fig. 7). The 0.7 pss decrease of SSS coincides with a rain event of 3.3 mm h^{-1}. Its associated 3d max rain rate is equal to 3.80 mm h^{-1}.

For a given 3d max rain rate, the vertical salinity differences observed locally by an autonomous drifter can be much higher than what our regression lines indicate. It must strengthen that freshening resulting from rain is often very local, involving a spatial scale much smaller than satellite pixels. Because local salinity was collocated with 25 km × 25 km pixel rainfall, these regressions are representative of freshening effect integrated over a satellite pixel; thus, they are much lower than local effect but probably close to the effect that will be observed on L-band radiometric pixels.

The future increase in salinity measurements at 50-cm depth should allow drawing statistics for the uppermost meters of the ocean. In future work, these estimates could be compared with theoretical model estimates, such as the Price et al. (1986) model. This one computes the salinity profile in cases of precipitation with a vertical sampling of several tenths of centimeters, whereas

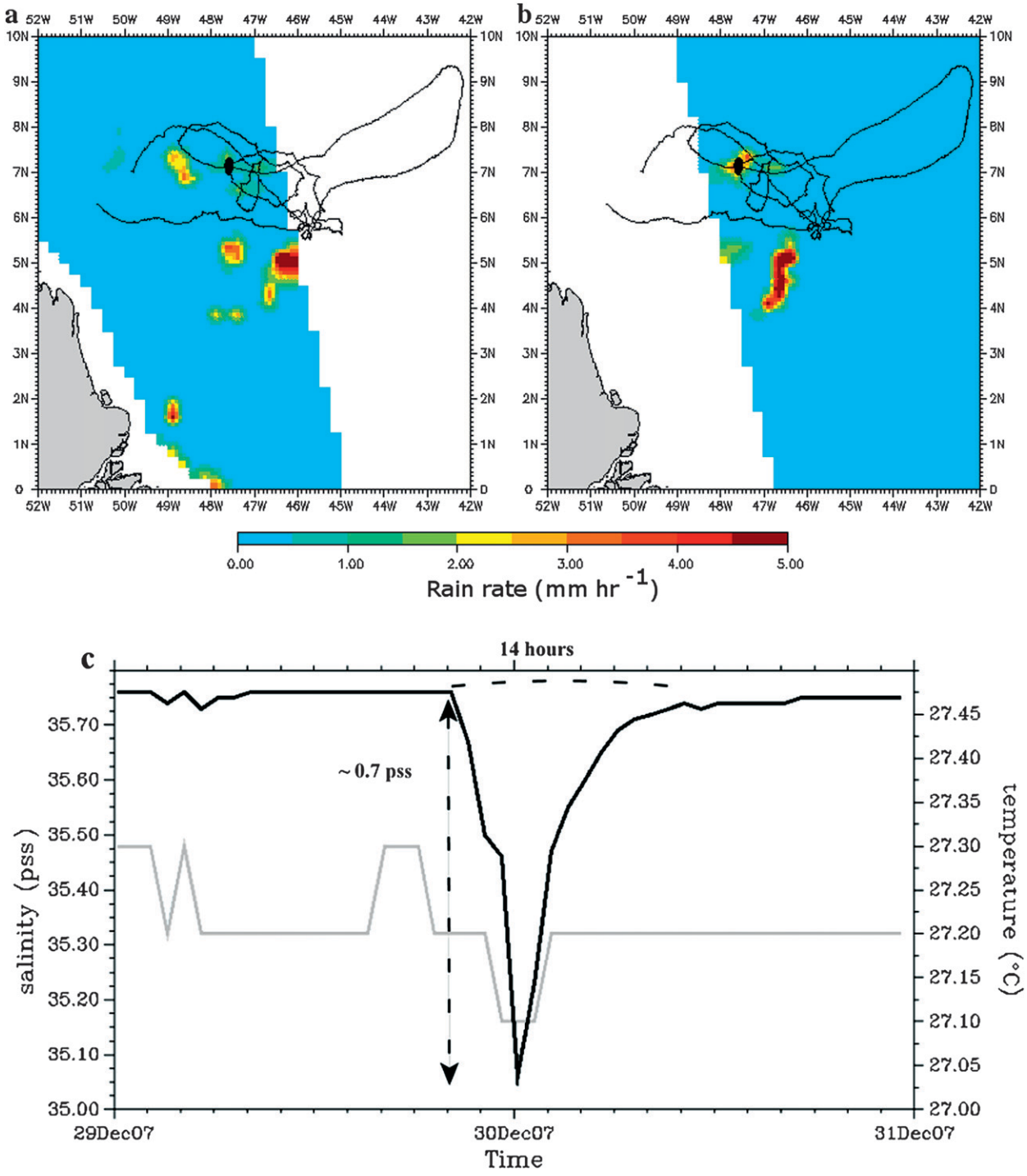

FIG. 7. Trajectory of the Metocean buoy superimposed on measurements of the rain rate made by (a) *F14* SSM/I satellite at nearly 2030 LT 29 Dec 2007 and (b) *F13* SSM/I satellite at nearly 2111 LT 29 Dec 2007. The dark curve represents the trajectory of the MetOcean drifter between its launch (28 Oct 2007) and the beginning of May 2008. The large dark dot represents its position on 29 and 30 Dec 2007. (c) The salinity decrease recorded by Metocean buoy at 7°N, 48°W. The back curve represents the salinity measured at 66-cm depth and the gray curve represents the temperature at 56-cm depth.

Schlüssel et al. (1997) compute the salinity decrease induced by rain events in the molecular sublayer of the ocean.

To document vertical salinity differences that can be expected from the occurrence of rain, we recommend using precipitation derived from satellite measurements and a statistical approach. With a 3d max rain rate superior to 10 mm h^{-1}, vertical salinity differences, all vertical levels combined, can reach on average more than 0.075 pss (see Fig. 5).

This approach, which is valuable only from a statistical point of view, is probably less accurate than physical models describing the penetration of rain in the ocean and the near-surface ocean circulation. However, these models need detailed atmospheric forcing (heat fluxes, wind speed, etc.) and modeling of ocean circulation (advection, etc.) that will not be easily available for all radiometric measurements.

6. Conclusions

Precipitation represents an important issue for the L-band radiometer. Vertical salinity gradients higher than 0.1 and up to 1 pss, which is consistent with strong rain events, are observed in tropical regions. These vertical salinity differences increase with the depth differences between the two measurements and are at maxima when 1-m depth measurements are considered. Careful studies about salinity vertical variability between the centimeter and 5-m depths in rainy regions are highly recommended. In addition, the fixed time passage of these satellites (0600 and 1800 LT) coincides with the precipitation maxima over ocean and land determined by Yang et al. (2008).

If the expected precision of satellite equals several tenths of a pss on average over space and time, rain events do not represent an obstacle. However, if this precision is fixed at less than 0.1–0.2 pss for an average computed over 10 days and 200 km $\times$ 200 km, rain events associated with mixing and surface currents can create a vertical salinity difference between L-band radiometer data and in situ data. In this case, the rain rate computed by satellites provides reliable information and correlation between salinity differences, and the 3d max rain rate as defined in this paper can be used.

Some recommendations can be drawn from this study to optimize calibration and validation of the L-band radiometer SSS measurements. First of all, a detailed and complete check of in situ measurements has to be done to avoid suspicious or averaged data. Next, agreeing with the recommendations of U.S. CLIVAR Office (2007), surface Argo salinity measurements shallower than 5 m are needed, and more measurements at the upper ocean surface, such as those performed at 15–30 cm by surface floats or the high-resolution vertical profiles performed up to 1 cm (Ho et al. 2004), have to be collected, particularly in the tropical band.

Acknowledgments. The authors are indebted to P. Blouch and J. Rolland of Meteo-France for providing support and assistance in the use of the Metocean buoy. They thank T. Delcroix, F. Gaillard, L. Barbero, and J. Gourrion for their scientific and technical advice; X. Yin for his rereading of this paper; and S. Le Reste and B. Bourles for their helpful explanation of the functioning of Argo floats. The authors wish to thank all the people participating in the Argo floats dissemination and the Argo technical and scientific team for providing free access to the Argo measurements. We also acknowledge G. Rohardt and all the R/V *Polarstern* team for their help and for providing data, the SISMER team and the TAO Project Office of NOAA/PMEL, T. Boyer and the National Oceanographic Data Center, Remote Sensing Systems, and NASA Earth Science REASoN DISCOVER Project for providing free and open access to TAO and PIRATA data; the World Ocean Database 2005; and measurements from SSM/I, TMI, and AMSR-E satellites, respectively. The authors are indebted to N. Martin for his computing support and valuable help. We are also gratefully acknowledged to three anonymous reviewers whose thoughtful comments significantly contributed to improvement of the manuscript.

This work is part of the Global Ocean Sea Surface Salinity Calibration and validation for SMOS (GLOSCAL) project and is supported by the French program CNES/TOSCA and by ESA. C. Henocq is supported by a CIFRE/CNRS/ACRI-St fellowship.

APPENDIX

Data Correction and Sorting

a. Salinity measurements

1) MEASUREMENTS FROM TAO/TRITON AND PIRATA MOORINGS

The selection of valid data is made according to the validation flags provided on the Web site. In addition, we perform a check on the consistency of vertical salinity profiles. In what follows, salinity measured at a depth of X meters will be noted SX_m. First, data with a validation flag equal to 4 (meaning low-quality data) are discarded, and the highest-quality data (validation flag equal to 1) are selected. Then, for default quality and adjusted data (validation flags equal to 2 and 3, respectively), the temporal variations of S5_m–S1_m, of

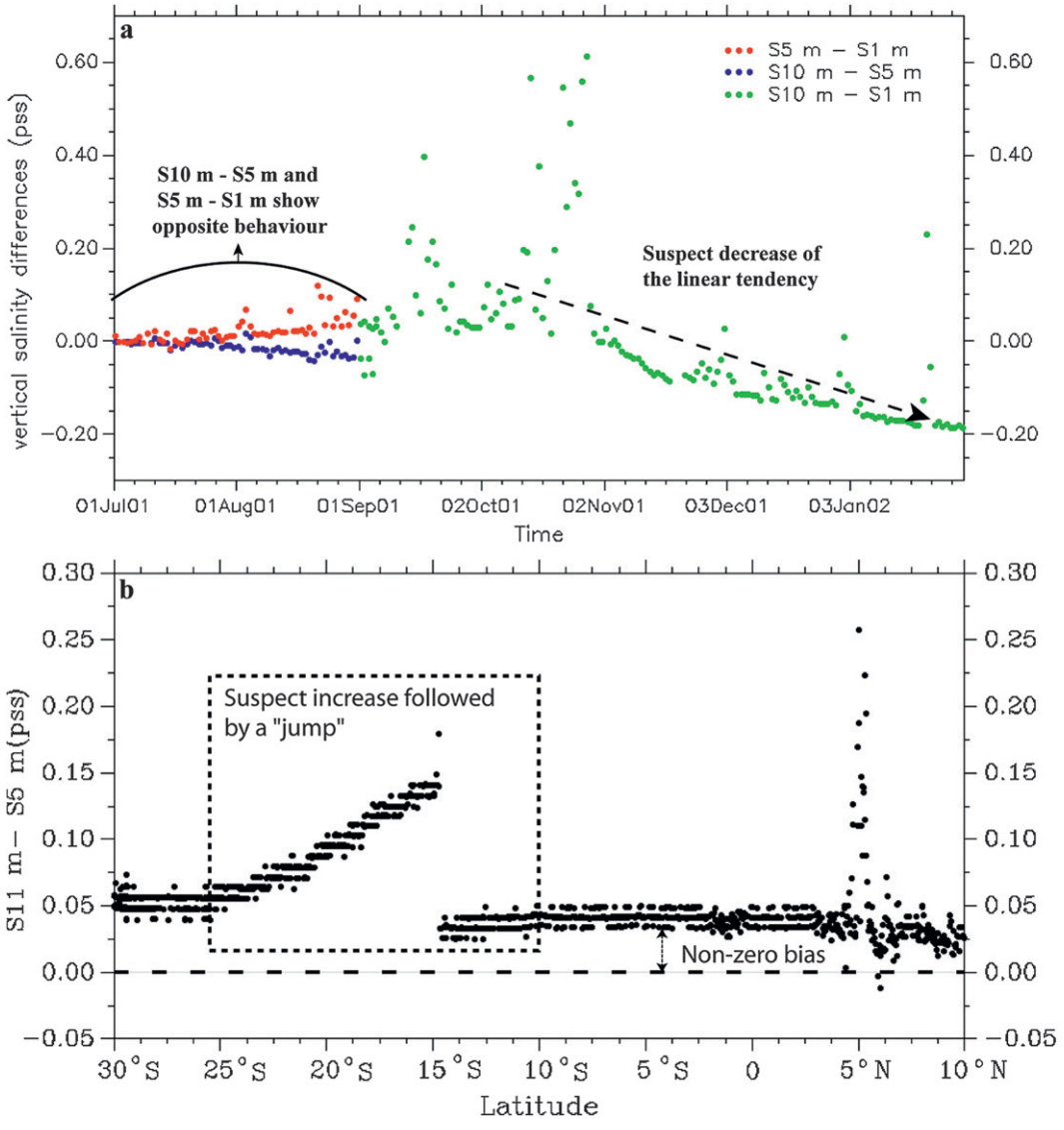

FIG. A1. Examples of problems encountered with salinity data measured at two depths. (a) The TAO mooring located at 12°N, 95°W, where red dots represent salinity differences measured between 5- and 1-m depths, blue dots represent the differences between 10- and 5-m depth, and green dots represent the differences between 10- and 1-m depths. All these measurements are discarded in this study. (b) *Polarstern*'s TSG in April 1997; this plot shows two problems of calibration met with *Polarstern*'s data: suspect increase and jump in vertical gradients (data from 25° to 15°S are discarded in this study) and nonzero bias (corrected by taking the 5-m depth measurements as the reference).

S10_m–S5_m, and of S10_m–S1_m are studied. When the linear trend of salinity differences shows a suspect slope or when S5_m–S1_m and S10_m–S5_m showed opposite behavior (see Fig. A1a), data are discarded. Selected data, after this sorting work, come from 13 sites located in the Pacific and Atlantic Oceans.

2) MEASUREMENTS FROM *POLARSTERN*

An important work of correction and selection of data is accomplished. Sometimes the *Polarstern* time series of S11_m–S5_m shows an important increase followed by a jump that are probably linked to TSG fouling and calibration problems (see Fig. A1b). This problem cannot be easily corrected, so these data are rejected. Some transects also present a suspect nonzero bias. Because the surface layer is expected to be homogeneous between 5 and 11 m most of the time, the median value of vertical differences calculated over a transect should be equal to zero. According to the *Polarstern* team (G. Rohardt 2006, personal communication), the 5-m sensor is calibrated more accurately than the 11-m sensor, so, for each transect separately, the conductivity measured

TABLE A1. Corrections applied to the different *Polarstern* transects.

Date of *Polarstern*'s transects	Correction applied (S m^{-1})	Date of *Polarstern*'s transects	Correction applied (S m^{-1})
October–November 1993	−0.130	May 1999	−0.006
June 1994	−0.170	December 1999	−0.273
October–November 1994	0.170	January 2000	−0.279
May 1995	−0.470	May–June 2000	−0.093
June 1996	0.005	January–February 2003	0.000
October 1996	0.000	October–November 2003	−0.032
April 1997	0.000	May 2004	0.000
October–November 1997	−0.004	October 2004	−0.047
December 1998	−0.014	June 2005	−0.090
January 1999	−0.019	October–November 2005	−0.087

at 11-m depth is adjusted to get a median of the conductivity difference between 5 and 11 m equal to zero. Table A1 summarizes the correction applied to each transect. This kind of problem does not appear with the temperature gradient.

3) MEASUREMENTS FROM ARGO FLOATS

Active Argo floats fall into three main different types: APEX floats (representing 65.2% of the active floats on 1 August 2008; information available online at http://argo.jcommops.org), Sounding Oceanographic Lagrangian Observer (SOLO) floats (28.1%), and Provor floats (5.3%). Depending on their type, for each measurement, floats transmit either depth-integrated conductivity measurements (SOLO and Provor) or an instantaneous measurement (APEX). Because salinity differences can be smoothed as a result of depth averaging, only APEX measurements from 1 January 2000 to 31 December 2006 are retained.

The selection of Argo data is made first in accordance with the Coriolis validation flags (Wong et al. 2008). Data with a flag equal to 1 or 2 (meaning good or probably good data) and salinity measurements greater than 20 pss are retained. Some Argo floats present salinity differences larger than 0.15 pss between two depths separated by less than 1 m. These floats, which are also considered inaccurate by J. Gourrion (2007, personal communication), are discarded.

4) MEASUREMENTS FROM CTD AND XCTD

The first verification deals with depth and salinity amplitude: many measurements above 4 m seemed suspicious (for instance, measurements smaller than 20 pss in the open ocean). As a consequence, only salinity measurements made after 1 January 2000 between 4 and 11 m and higher than 20 pss are retained. Concerning WOD05, validation flags provided by the data submitters are taken into account to retain only good and probably good data. When these flags are not available, the selection is based on a quality-control flag computed by the WOD05 team using statistical methods. Concerning the SISMER database, measurements made after 1 January 2000 between 4 and 11 m and flagged as good (quality flag equal to 1) or probably good (quality flag equal to 2) are retained. Data from the ARAMIS project are processed by the ARAMIS team, and only measurements below 4-m depth are considered.

Less than 280 000 vertical salinity differences are obtained over the entire tropical region, divided into three verticals levels: ΔS_{10-5}, ΔS_{5-1}, and ΔS_{10-1}. The different zones sampled by the distinct types of data are drawn in Fig. A2. Table A2 indicates the different distributions according to the data type, the vertical level, and the geographical position. The time series extends from 1993 to 2006, but data before January 2000 come only from the *Polarstern*.

b. Rain and surface wind speed measurements

For each satellite, SSM/I, TMI, AMSR-E, and QuikSCAT, the rain rate and surface wind speed product is provided on two maps for each day at 0.25° resolution, corresponding to ascending and descending orbits, with different spatial and temporal coverage. For each satellite, surface wind speed corresponds to wind speed 10 m above the water surface, derived from surface roughness.

- From 1987, several SSM/I satellites have been launched. Each day, two passes between 80°N and 80°S, called ''morning pass'' and ''evening pass,'' are registered. Satellites pass overhead at approximately the same local time each evening or morning; this time passage alters slightly over the course of the year. For SSM/I satellites, five of them overlap in time with computed vertical salinity differences (see Table A3).
- TMI data are provided in the form of daily maps separated into ascending and descending orbit segments. The data are available from 7 December 1997. They cover a region from 40°S to 40°N. Unlike SSM/I

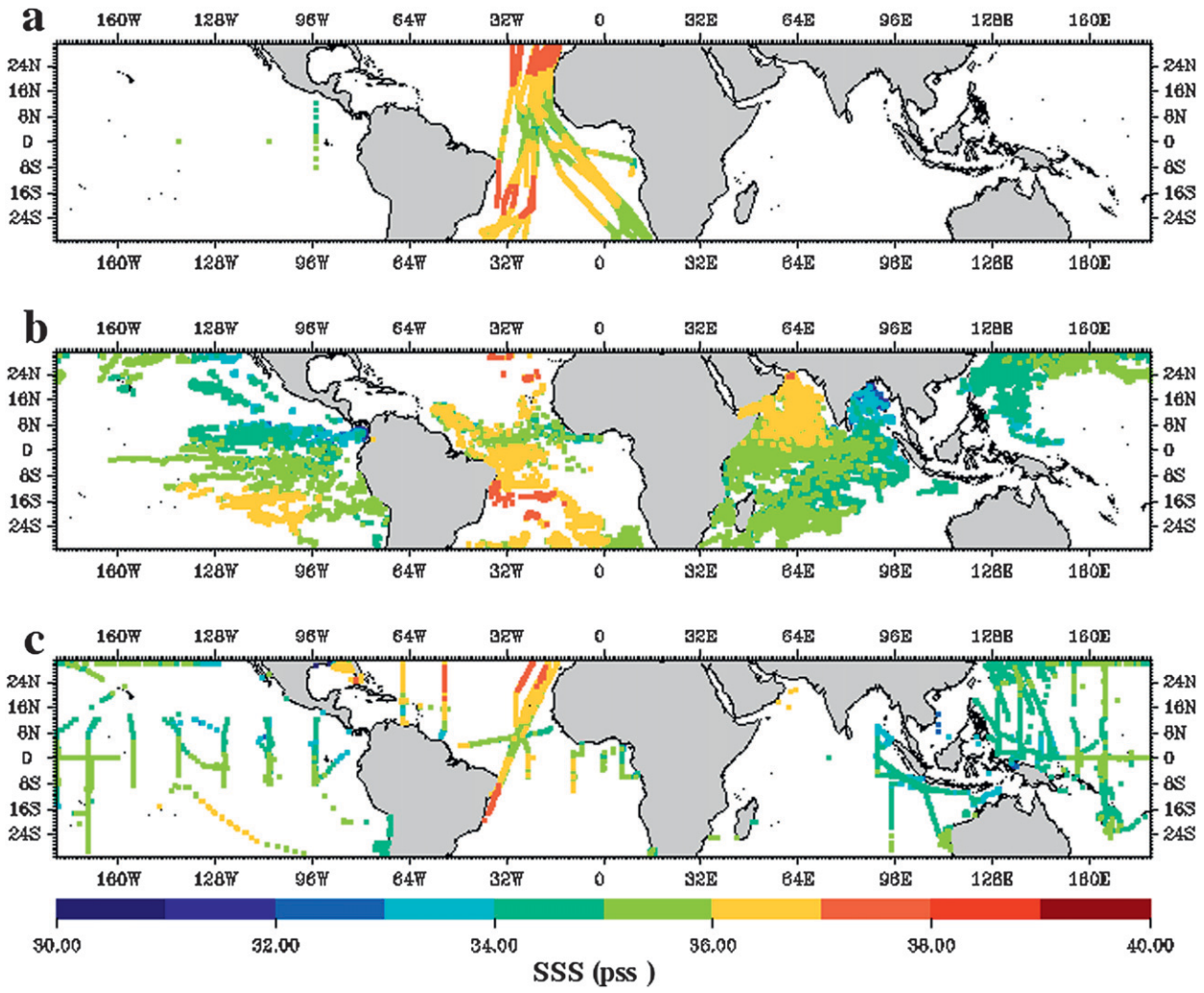

FIG. A2. Positions of measurements made (a) on TAO/PIRATA moorings or by TSG on boats (we take only those boats with two measurements in the first 10 m), (b) by Argo floats, and (c) by CTD and XCTD (from WOD05, SISMER, and ARAMIS project). Colors represent the shallowest measurement salinity of each profile. When several values of SSS occur at the same point, only the highest value is displayed.

satellites, the TMI satellite travels west–east in a semi-equatorial orbit and does not record data at the same local time.

- The AMSR-E on board the *Aqua* spacecraft has provided validated data since 1 June 2002. The local equator crossing time is 1330 LT for the ascending pass and 0130 LT for the descending pass, and the spatial coverage extends from 80°N to 80°S.
- The microwave scatterometer QuikSCAT has provided data since July 1999.

Each vertical salinity difference is collocated with rain rate computed by these satellites over the previous 72 h in 25-km radii, to calculate their associated 3d max rain rate, and with maximum surface wind speed over the previous hour in 25 km radii, to calculate their associated 1hr_WS.

c. *Sorted dataset*

To detect biased and wrong measurements, the combined dataset (i.e., vertical salinity differences with their associated 3d max rain rate) is sorted into groups of 3d max rain rate (from 0 to 1 mm h^{-1}, from 1 to 2 mm h^{-1}, and so on, until greater than 10 mm h^{-1}, with each group being composed of more than 30 salinity measurements). In each group, the mean and the standard deviation (denoted as M and STD, respectively) of salinity differences are calculated. We choose to discard data outside the interval [M ± 5 STD].

TABLE A2. Distribution of the salinity differences according to the type of data, the vertical level, and the geographical location.

	Distribution in the dataset
Data type	
TAO/PIRATA and *Polarstern* measurements	88.0% (76.0% from TAO/PIRATA)
Argo measurements	9.1%
CTD-XCTD measurements from WOD05, SISMER, and ARAMIS project	2.9%
Vertical level	
ΔS_{10-5}	46.5%
ΔS_{5-1}	30.9%
ΔS_{10-1}	22.6%
Geographical location	
Atlantic Ocean	14.4%
Pacific Ocean	80.7%
Indian Ocean	4.9%

Except for some large differences in the eastern Pacific and in the Indian Ocean, they are actually located near coastlines or mouths of rivers such as the Amazon or the Niger. In addition, a comparison of the shallowest temperature versus shallowest salinity diagram (T–S diagram) for discarded profiles and for the whole dataset shows that the discarded salinity differences have a warmer SST and lower SSS than the majority of the dataset. This indicates that these profiles are mostly sampled in river plumes (Del Vecchio and Subramaniam 2004) and that they correspond to large vertical salinity differences that sometimes appear near the coast because of river discharge.

The primary goal of SMOS is to retrieve salinity in the open ocean and because radiometric measurements are strongly contaminated by the presence of coastlines, which is because the emissivity of land is about twice as large as that of the ocean (Zine et al. 2007), calibration and validation of SMOS SSS measurements will not put much emphasis on coastal areas. As a consequence, discarding data outside the interval [M ± 5 STD] appears to be justified.

TABLE A3. Time availability of SSM/I satellites. Only satellites consistent with computed salinity differences are displayed.

SSM/I satellites consistent with computed salinity differences	Date of first measurement	Date of last measurement
F10	8 Dec 1990	14 Nov 1997
F11	3 Dec 1991	16 May 2000
F13	3 May 1995	Still working
F14	8 May 1997	Still working
F15	18 Dec 1999	13 Aug 2006

REFERENCES

Arnault, S., N. Chouaib, D. Diverres, S. Jacquin, and O. Coze, 2004: Comparison of TOPEX/Poseidon and Jason altimetry with ARAMIS in situ observations in the tropical Atlantic Ocean. *Mar. Geod.,* **27,** 15–30.

Barre, H. M. J. P., B. Duesmann, and Y. Kerr, 2008: SMOS: The mission and the system. *IEEE Trans. Geosci. Remote Sens.,* **46,** 587–593.

Bingham, F. M., S. D. Howden, and C. J. Koblinsky, 2002: Sea surface salinity measurements in the historical database. *J. Geophys. Res.,* **107,** 8019, doi:10.1029/2000JC000767.

Boutin, J., and N. Martin, 2006: ARGO upper salinity measurements: Perspectives for L-band radiometers calibration and retrieved sea surface salinity validation. *Geosci. Remote Sens. Lett.,* **3,** 202–206.

——, P. Waldteufel, N. Martin, G. Caudal, and E. Dinnat, 2004: Surface salinity retrieved from SMOS measurements over global ocean: Imprecisions due to surface roughness and temperature uncertainties. *J. Atmos. Oceanic Technol.,* **21,** 1432–1447.

Boyer, T. P., and Coauthors, 2006: *World Ocean Database 2005*. S. Levitus, Ed., NOAA Atlas NESDIS 60, 190 pp.

Cronin, M. F., and M. J. McPhaden, 1999: Diurnal cycle of rainfall and surface salinity in the western Pacific warm pool. *Geophys. Res. Lett.,* **26,** 3465–3468.

Delcroix, T., M. McPhaden, A. Dessier, and Y. Gouriou, 2005: Time and space scales for sea surface salinity in the tropical oceans. *Deep-Sea Res. I,* **52,** 787–813.

Del Vecchio, R., and A. Subramaniam, 2004: Influence of the Amazon River on the surface optical properties of the western tropical North Atlantic Ocean. *J. Geophys. Res,* **109,** C11001, doi:10.1029/2004JC002503.

Elliott, G. W., 1974: Precipitation signatures in sea-surface-layer conditions during BOMEX. *J. Phys. Oceanogr.,* **4,** 498–501.

Font, J., G. S. E. Lagerloef, D. M. LeVine, A. Camps, and O. Z. Zanifé, 2004: The determination of surface salinity with the European SMOS space mission. *IEEE Trans. Geosci. Remote Sens.,* **42,** 2196–2205.

Gould, J., and Coauthors, 2004: Argo profiling floats bring new era of in situ ocean observations. *Eos, Trans. Amer. Geophys. Union,* **85,** doi:10.1029/2004EO190002.

Ho, D. T., C. J. Zappa, W. R. McGillis, L. F. Bliven, B. Ward, J. W. H. Dacey, P. Schlosser, and M. B. Hendricks, 2004: Influence of rain on air-sea gas exchange: Lessons from a model ocean. *J. Geophys. Res.,* **109,** C08S18, doi:10.1029/2003JC001806.

Hsiao, M., S. Lichter, and L. G. Quintero, 1988: The critical Weber number for vortex and jet formation for drops impinging of a liquid pool. *Phys. Fluids,* **31,** 3560–3562.

Lagerloef, G. S. E., C. F. Swift, and D. M. L. Vine, 1995: Sea surface salinity: The next remote sensing challenge. *Oceanography,* **8,** 44–50.

Le Vine, D. M., G. S. E. Lagerloef, F. R. Colomb, S. H. Yueh, and F. A. Pellerano, 2007: Aquarius: An instrument to monitor sea surface salinity from space. *IEEE Trans. Geosci. Remote Sens.,* **45,** 2040–2050.

McPhaden, M. J., 1995: The tropical atmosphere-ocean array is completed. *Bull. Amer. Meteor. Soc.,* **76,** 739–741.

Miller, J. R., 1976: The salinity effect in a mixed layer ocean model. *J. Phys. Oceanogr.,* **6,** 29–35.

Ostapoff, F., Y. Tarbeyev, and S. Worthem, 1973: Heat flux and precipitation estimates from oceanographic observations. *Science,* **180,** 960–962.

Peichl, M., V. Wittmann, E. Anterrieu, B. Picard, N. Skou, and S. Sobjaerg, 2005: Final report: Scientific inputs for the SMOS level 1 processor development. ESA Contract 10508/02/NL/GS, 126 pp.

Price, J. F., 1979: Observation of a rain-formed mixed layer. *J. Phys. Oceanogr.,* **9,** 643–649.

——, R. A. Weller, and R. Pinkel, 1986: Diurnal cycling: Observations and models of the upper ocean response to diurnal heating, cooling, and wind mixing. *J. Geophys. Res.,* **91** (C7), 8411–8427.

Reverdin, G., P. Blouch, J. Boutin, P. P. Niiler, J. Rolland, W. Scuba, A. Lourenco, and A. F. Rios, 2007: Surface salinity measurements—COSMOS 2005 experiment in the Bay of Biscay. *J. Atmos. Oceanic Technol.,* **24,** 1643–1654.

Riser, S. C., L. Ren, and A. Wong, 2008: Salinity in ARGO. *Oceanography,* **21,** 56–67.

Schlüssel, P., A. V. Soloviev, and W. J. Emery, 1997: Cool and freshwater skin of the ocean during rainfall. *Bound.-Layer Meteor.,* **82,** 437–472.

Schmitt, R. W., 2008: Salinity and the global water cycle. *Oceanography,* **21,** 12–19.

Servain, J., A. J. Busalacchi, M. J. McPhaden, A. D. Moura, G. Reverdin, M. Vianna, and S. E. Zebiak, 1998: A Pilot Research Moored Array in the Tropical Atlantic (PIRATA). *Bull. Amer. Meteor. Soc.,* **79,** 2019–2031.

Soloviev, A., and R. Lukas, 1997: Observation of large diurnal warming events in the near-surface layer of the western equatorial Pacific warm pool. *Deep-Sea Res. I,* **44,** 1055–1076.

U.S. CLIVAR Office, 2007: Report of the U.S. CLIVAR Salinity Science Working Group. U.S. CLIVAR Rep. 2007-1, 50 pp. [Available online at http://www.usclivar.org/Pubs/Salinity_final_report.pdf.]

Ward, B., R. Wanninkhof, P. J. Minnett, and M. J. Head, 2004: SkinDeEP: A profiling instrument for upper-decameter sea surface measurements. *J. Atmos. Oceanic Technol.,* **21,** 207–222.

Wentz, F. J., and R. W. Spencer, 1998: SSM/I rain retrievals within a unified all-weather ocean algorithm. *J. Atmos. Sci.,* **55,** 1613–1627.

Wijesekera, H. W., C. A. Paulson, and A. Huyer, 1999: The effect of rainfall on the surface layer during a westerly wind burst in the western equatorial Pacific. *J. Phys. Oceanogr.,* **29,** 612–632.

Wong, A., R. Keeley, T. Carval, and A. D. M. Team, 2008: Argo quality control manual, version 2.4. Argo Data Management ar-um-04-01, 35 pp. [Available online at http://www.coriolis.eu.org/cdc/argo/argo-quality-control-manual.pdf.]

Yang, S., K. Kuo, and E. A. Smith, 2008: Persistent nature of secondary diurnal modes of precipitation over oceanic and continental regimes. *J. Climate,* **21,** 4115–4131.

Yueh, S. H., R. West, W. J. Wilson, K. K. Li, E. G. Njoku, and Y. Rahmat-Samii, 2001: Error sources and feasibility for microwave remote sensing of ocean surface salinity. *IEEE Trans. Geosci. Remote Sens.,* **39,** 1049–1060.

Zine, S., J. Boutin, P. Waldteufel, J. L. Vergely, T. Pellarin, and P. Lazure, 2007: Issues about retrieving sea surface salinity in coastal areas from SMOS data. *IEEE Trans. Geosci. Remote Sens.,* **45,** 2061–2072.

——, and Coauthors, 2008: Overview of the SMOS sea-surface-salinity prototype processor. *IEEE Trans. Geosci. Remote Sens.,* **46,** 621–645.